

Supporting Information for

A New Compound Pt₃Bi₂S₂ with Superior Performance for Hydrogen Evolution Reaction

Yuqiang Fang^{a,+}, Sishun Wang^{a,+}, Gaoxin Lin,^a Xin Wang^{c,}, Fuqiang Huang^{a,b*}*

List of contents

- 1. Experimental section.**
- 2. Supplementary Figures.**
- 3. Supplementary Tables.**

1. Experimental section.

Reagents.

All starting materials were obtained from Aladdin and stored in a glove box filled with Ar. Bismuth (powder, 99%), platinum (powder, 99.9%) and sulfur (powder, 99.5%) were used without further purification.

Synthesis of $\text{Pt}_3\text{Bi}_2\text{S}_2$.

Single crystals of $\text{Pt}_3\text{Bi}_2\text{S}_2$ were synthesized *via* solid-state reaction from a mixture of Pt powder, Bi powder, and S powder. A mixture of Pt powder (0.1951 g, 1 mmol), Bi powder (0.2090 g, 1 mmol) and S powder (0.0214 g, 0.67 mmol) was loaded into a carbon-coated fused silica tube. The tube was then flame-sealed under vacuum (1×10^{-3} mbar), and heated slowly to 1223 K in a programmable furnace. The tube was kept at this temperature for 2 days, and then slowly cooled to 573 K at the rate of 1 K h^{-1} . Then, the furnace was turned off to cool to room temperature. The tube was cracked and the black crystals of $\text{Pt}_3\text{Bi}_2\text{S}_2$ were obtained.

The pure sample of $\text{Pt}_3\text{Bi}_2\text{S}_2$ was prepared by Pt powder (0.2927 g), Bi powder (0.2299 g) and S powder (0.03531 g) at 873 K for 1 day.

Single crystal X-ray crystallography.

High-quality crystals of $\text{Pt}_3\text{Bi}_2\text{S}_2$ were chosen from the as-prepared samples and mounted on a glass fiber for single-crystal X-ray diffraction. Data collection was performed on a Bruker D8 Quest CCD diffractometer equipped with graphite-monochromated $\text{Mo } K_\alpha$ radiation at 297K. The structure was solved with direct methods built in the program SHELXS integrated in the Apex 3 suite, and refined with the full-matrix least-squares method using the SHELXL-2014 program^[1]. The crystallographic data and refinement details for $\text{Pt}_3\text{Bi}_2\text{S}_2$ are summarized in **Table S2** and selected bond distances and bond angles are presented in **Table S3**. The CSD number of $\text{Pt}_3\text{Bi}_2\text{S}_2$ is 2084111.

Characterization.

The as-synthesized crystal samples were ground into fine powders before use. The powder X-ray diffraction pattern was collected on a Bruker D2 Phaser X-ray diffractometer ($\text{Cu } K_\alpha$, $\lambda = 1.5406 \text{ \AA}$). Simulated patterns were generated using the FullProf program and the CIF file from single crystal structure determination. The morphology and elemental composition of $\text{Pt}_3\text{Bi}_2\text{S}_2$ were investigated with a JEOL (JSM6510) scanning electron microscope and a JEM-2100F transmission electron microscope. The valence analysis of the samples was obtained from X-ray photoelectron spectroscopy (XPS) carried out on the RBD upgraded PHI- 5000C ESCA system (PerkinElmer) with $\text{Mg } K_\alpha$ radiation ($h\nu = 51253.6 \text{ eV}$). The binding energies in XPS analysis were corrected by referencing C 1s peak at 284.6 eV. The valence band level obtained by ultraviolet photoemission spectroscopy (UPS) with a ThermoFisher ESCALAB 250XI instrument using He ($h\nu = 21.21 \text{ eV}$). The resistivities of the as-prepared compounds were measured a Quantum Design Physical Properties Measurement System (PPMS-9T, Quantum Design Company). As for the resistivity measurement, a four-probe method was adopted. Silver paste and copper wire were acted as the contact electrode and conduct wire, respectively.

Electronic Structure Calculation.

The first principles computations based on density functional theory (DFT) were performed using the VASP package. The Perdew–Burke–Ernzerhof (PBE) version of the generalized gradient approximation (GGA) was used to describe the exchange correlation functional, and the linearized augmented plane wave (LAPW) method (PAW) method was used in the present work. Here, the cutoff energy of plane wave was chosen at 480 eV. For the density of states (DOS) calculations of Pt₃Bi₂S₂, 8 × 8 × 8 k-points were used for the conventional cell. The convergence criteria were that the change in total energies between two successive electronic steps was less than 10⁻⁵ eV, and all the Hellmann-Feynman force acting on each atom was less than 0.01 eV /Å. High-symmetry points in the Brillouin zone (H, G, P and PA represent (0.5, -0.5, 0.5), (0.0, 0.0, 0.0), (0.25, 0.25, 0.25), and (-0.25, -0.25, 0.75) points) were considered in our band structure calculation. The DOS of PtS₂ are calculated by 4 × 4 supercell with 3 × 3 × 1 k-points sampling and DOS of Pt (111) are modeled by a 2 × 2 super cell with four layers.

Electrochemical measurements.

All electrochemical measurements were performed on a three-electrode configuration using rotating disk electrode (RDE) coating with a film of catalyst as the working electrode, saturated calomel electrode (SCE) as the reference electrode and graphite rod as the counter electrode. HER measurements were conducted in Ar-saturated 0.5 M H₂SO₄. All the data were recorded by a CHI660E Electrochemical Workstation (Chenhua, Shanghai). Before test, the Pt₃Bi₂S₂ and PtS₂ were treated with ball milling for 4 hours by using a Fritsch Pulverisette 7 apparatus to reduce the particle size. The catalysts were dispersed in Nafion/alcohol solution (0.5 wt. %, Alfa Aesar) by sonication for 60 min to form 10 mg mL⁻¹ slurry. 15 μL of above slurry was pipetted onto the polished RDE in order to obtain a film of catalyst (loading mass of 0.76 mg cm⁻²). Hydrogen evolution performances were evaluated by the linear sweep voltammetry at scan rate of 10 mV s⁻¹ with iR compensation of 90%. The ECSA was measured by using the equation $ECSA = C_{dl}/C_s$, where the electrochemical double layer capacitance (C_{dl}) was determined by CV curves at different scan rates and the general specific capacitance (C_s) was 0.035 mF cm⁻² in 0.5 M H₂SO₄. Electrochemical impedance spectroscopy (EIS) was obtained at the potential of 10 mA cm⁻² with amplitude of 5 mV and frequency range of 0.1 Hz~10⁵ Hz. The potential was converted to reversible hydrogen electrode (RHE) according to the formula: $E(RHE) = E(SCE) + 0.0592 \times pH$.

2. Supplementary figures.

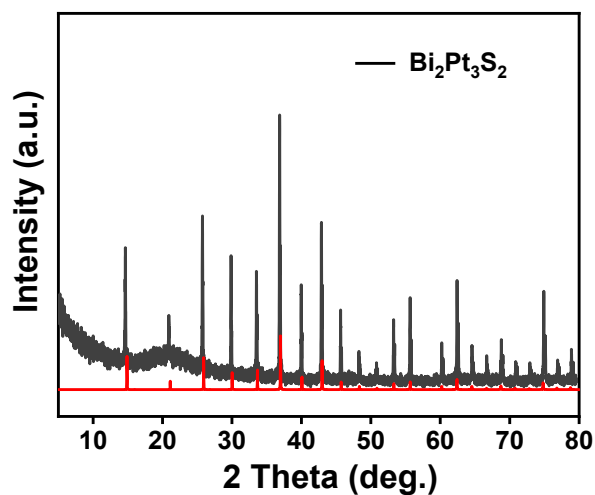


Figure S1. XRD pattern of the Pt₃Bi₂S₂ powder.

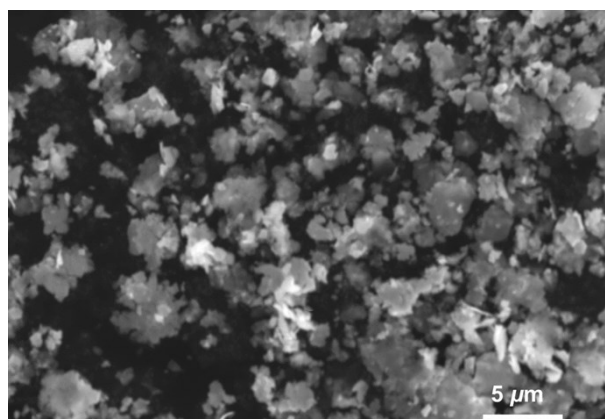


Figure S2. Low-magnification SEM image of Pt₃Bi₂S₂ sample.

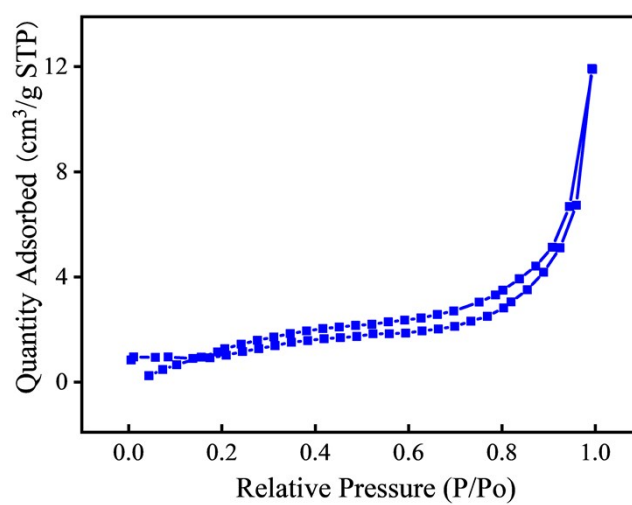


Figure S3. Nitrogen absorption-desorption isotherms curves of Pt₃Bi₂S₂ sample.

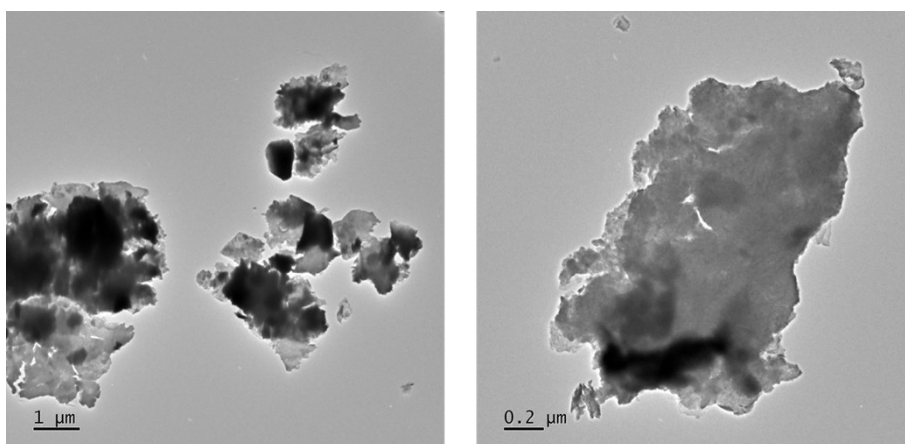


Figure S4. Low-magnification TEM image of $\text{Pt}_3\text{Bi}_2\text{S}_2$ particles.

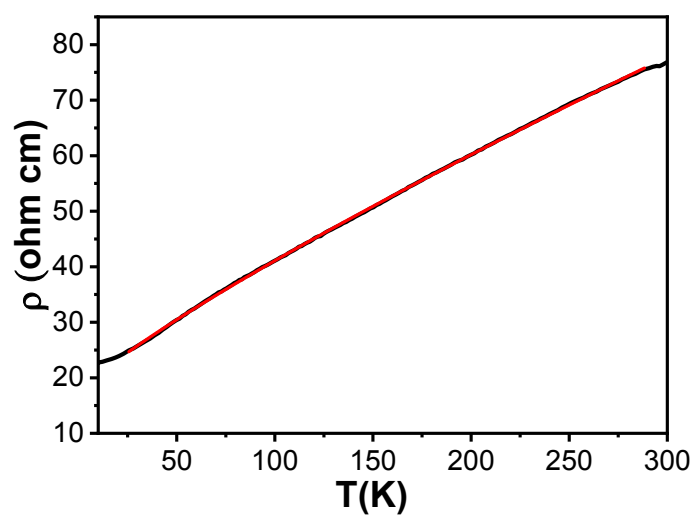


Figure S5. Temperature dependence of resistivity of $\text{Bi}_2\text{Pt}_3\text{S}_2$.

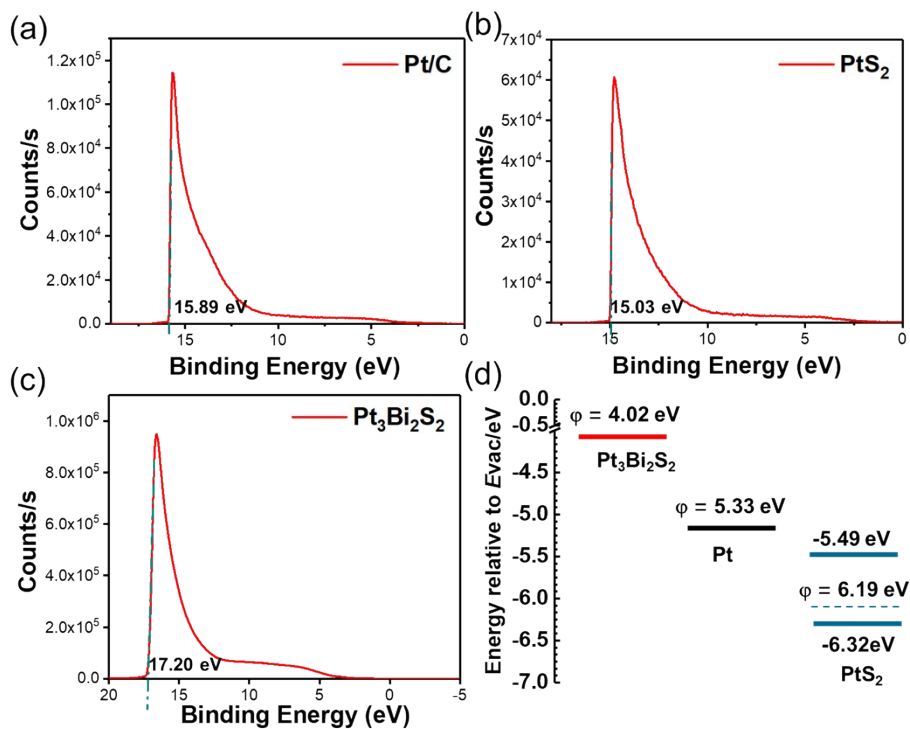


Figure S6. Ultraviolet photoelectron spectroscopy (UPS) of (a) Pt/C, (b) PtS₂ and (c) Pt₃Bi₂S₂; (d) Work functions of Pt/C, PtS₂ and Pt₃Bi₂S₂.

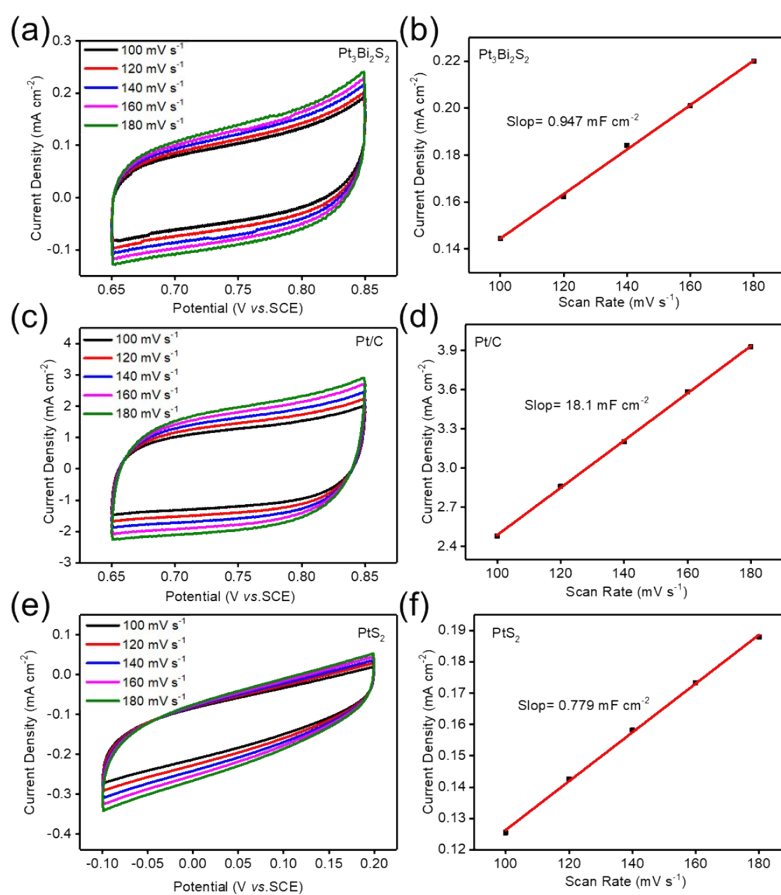


Figure S7. CV curves at different scan rates. (a) $\text{Pt}_3\text{Bi}_2\text{S}_2$, (c) Pt/C, (e) PtS_2 ; Electric capacities calculated by the electricity data in different scan rates; (b) $\text{Pt}_3\text{Bi}_2\text{S}_2$, (d) Pt/C, (f) PtS_2 .

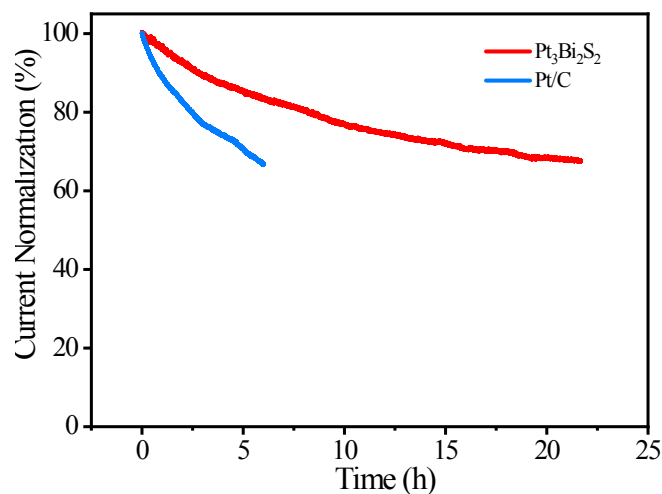


Figure S8. I/t curves of $\text{Pt}_3\text{Bi}_2\text{S}_2$ and Pt/C sample after cycling for several hours.

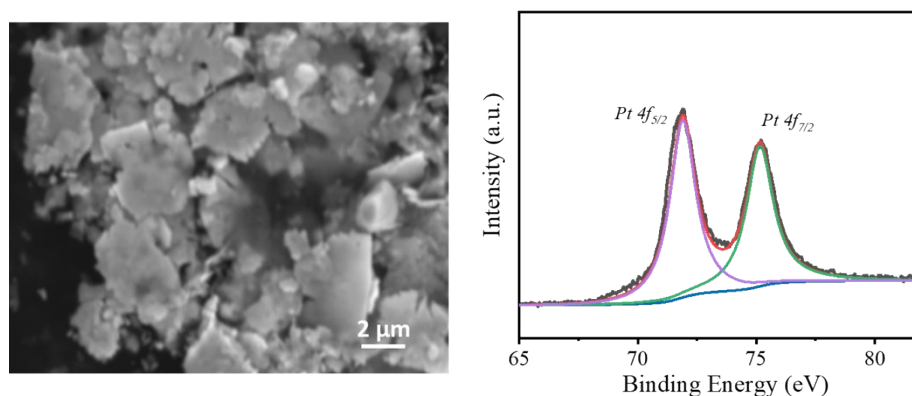


Figure S9. a) SEM image of the $\text{Pt}_3\text{Bi}_2\text{S}_2$ sample after HER cycling. b) X-ray photoelectron spectra of $\text{Pt}_3\text{Bi}_2\text{S}_2$ after HER cycling.

3. Supplementary tables.

Table S1. Crystallographic Data and Details of the Structure Refinements of $\text{Pt}_3\text{Bi}_2\text{S}_2$

Empirical formula	$\text{Pt}_3\text{Bi}_2\text{S}_2$
Formula weight (g/mol)	1067.32
Space group	$I2_13$
Crystal system	Cubic
unit cell	$a = 8.4111(16) \text{ \AA}$
Volume (\AA^3)	595.1(3)
Z	4

$F(000)$	1728
Radiation type	Mo K_{α}
$\mu(\text{mm}^{-1})$	129.77
Crystal size (mm)	0.05 x 0.04 x 0.01
T_{\min}, T_{\max}	0.003, 0.273
Reflections collected	4477
Independent reflections	179
Calculated density (g/cm^3)	11.913
crystal color	Black
Goodness-of-fit on F^2	1.18
R_{int}	0.067
R_1 for $[I > 2\sigma(I)]^a$	0.011
wR_2 for $[I > 2\sigma(I)]^a$	0.026

^a $R1 = \Sigma||F_o| - |F_c||/\Sigma|F_o|$, $wR_2 = [\Sigma w(F_o^2 - F_c^2)^2/\Sigma(wF_o^2)^2]^{1/2}$, $w = 1/[\sigma^2(F_o^2) + (aP)^2 + bP]$, where F_o is the observed structure factor, F_c is the calculated structure factor, σ is the standard deviation of F_c^2 , and $P = (F_o^2 + 2F_c^2)/3$. $S = [\Sigma w(F_o^2 - F_c^2)^2/(n - p)]^{1/2}$, where n is the number of reflections and p is the total number of parameters refined.

Table S2. EDS results of $\text{Pt}_3\text{Bi}_2\text{S}_2$

Element	Weight %	Atomic %
Pt	54.06	41.44
Bi	39.50	28.50
S	6.44	30.06
Totals	100.00	100.00

Table S3. The fitted parameters for $\text{Pt}_3\text{Bi}_2\text{S}_2$, PtS_2 , and Pt/C based on the EIS data.

Materials	R_s	R_{ct}	C_{dl}
PtS_2	25	51.42	5.1027×10^{-6}
$\text{Pt}_3\text{Bi}_2\text{S}_2$	19.3	11.35	6.0153×10^{-5}
Pt/C	6.091	0.37155	3.5388×10^{-3}